



POLITECNICO DI TORINO
Repository ISTITUZIONALE

CFD simulation of nanofiber-enhanced air filter media

Original

CFD simulation of nanofiber-enhanced air filter media / Tronville P.; Augusto L.L.X.; Bortolassi A.C.C.; Lopes G.C.; Gonçalves J.A.S; Rivers R.D.. - ELETTRONICO. - USB-Stick(2015), pp. 1-13. ((Intervento presentato al convegno FILTECH 2015 tenutosi a Cologne nel 24-26 February 2015.

Availability:

This version is available at: 11583/2607558 since:

Publisher:

Filtech Exhibitions Germany

Published

DOI:

Terms of use:

openAccess

This article is made available under terms and conditions as specified in the corresponding bibliographic description in the repository

Publisher copyright
default_conf_editorial

-

(Article begins on next page)

Plenary Lecture

How Could Integrated Science change the Separation Technology in the Future?

Dr. Karsten Keller
DuPont
USA

PL Tuesday, February 24, 2015
10:45-12:00 h

"The global population is project to grow from 7 billion today to 9 billion by 2050. The increase in population and the accompanying shifting global economic patterns will result in a significant increase in demand for food, energy and protection. Separation technology plays a key role in ensuring new solutions are environmentally sustainable. Indeed, existing separation technology has enabled us today to have clean air and water. Nearly every production process in today's society requires a separation step. As a result, global market in separation technology is growing and is over USD 100 billion annually. Exactly how should separation research develop in the next decade and beyond? Nowadays technical solutions are available for almost every separation task. However for the future the pressing challenge is to find economical solutions. If the ideal separation technology/process would have been invented, our world would face fewer difficulties for food, water, energy and environment..."

Keynote Lectures

Sugar Purification from Enzymatic Hydrolysis Products using Membrane Diafiltration

Prof. Kuo-Jen Hwang
Tamkang University, Dept. of Chemical and Materials Engineering, Taiwan

K1 Tuesday, February 24, 2015
13:00-14:15 h

Selective recovery of valuable plant and biomass compounds through biological membranes exposed to pulsed electric field: A new way for "green" filtration and purification technologies

Prof. Eugène Vorobiev
Université de Technologie de Compiègne, France

K2 Tuesday, February 24, 2015
14:45-16:00 h

Precoat Filtration. Insights into a well-established technology that still offers plenty of opportunities

Dr. Eberhard Gerdes
JRS Rettenmaier & Söhne
Germany

K3 Tuesday, February 24, 2015
16:45-18:00 h

Measuring Filter Cut Points and Pore Size Distributions by Challenge Testing

Dr. Graham Rideal
Whitehouse Scientific
UK

K4 Wednesday, February 25, 2015
09:00-10:15 h

Filtration – A Multi-Scale and Multi-Physics Challenge for Simulation

Dr. Martin Lehmann
Mann+Hummel
Germany

K5 Wednesday, February 25, 2015
10:45-12:00 h

On local Cake Properties in Liquid Filtration

Prof. Hans Theliander
Chalmers University of Technology, Forest Products and Chemical Engineering, Sweden

K6 Wednesday, February 25, 2015
13:00-14:15 h



Session Overview

Monday, 23.02.2015

09:00 – 18:00	Short Course I – Solid/Liquid Separation	Short Course II – Fine Dust Separation
---------------	--	--

Tuesday, 24.02.2015

08:30 – 10:15	Registration					
10:15 – 10:45	Opening Session					
10:45 – 12:00	PL Plenary Lecture – Dr. Karsten Keller, DuPont, USA How could Integrated Science change the Separation Technology in the Future?					
12:00 – 13:00	Lunch – Fair					
13:00 – 14:15	K1 Keynote Lecture 1 Prof. Kuo-Jen Hwang	L1 Dispersion Separation Analysis	L2 Cake Filtration-Analysis	G1 Surface Filtration I	G2 Gaseous, Liquid, Solid Contaminants	
14:15 – 14:45	Coffee Break – Fair					
14:45 – 16:00	K2 Keynote Lecture 2 Prof. Eugene Vorobiev	L3 Decanter Centrifuges and Hydrocyclones	L4 Cake Filtration-Washing	G3 Surface Filtration II	G4 Automotive Application	
16:00 – 16:45	Coffee Break – Fair					
16:45 – 18:00	K3 Keynote Lecture 3 Dr. Eberhard Gerdes	L5 Filtration Analysis, Apparatus, Selection & Design	L6 Continuous Vacuum and Pressure Cake Filters	G5 Surface Filtration III	M1 New Membranes	
18:00	Get Together Reception					

Wednesday, 25.02.2015

09:00 – 10:15	K4 Keynote Lecture 4 Dr. Graham Rideal	L7 Backwash Filters	G6 Modelling and Simulation	M2 Micro- and Ultrafiltration		
10:15 – 10:45	Coffee Break – Fair					
10:45 – 12:00	K5 Keynote Lecture 5 Dr. Martin Lehmann	L8 Vibration, Magnetic & Electric Enhanced Filtration	G7 Test Systems and Measurements	M3 Fouling and Scaling		
12:00 – 13:00	Lunch – Fair					
13:00 – 14:15	K6 Keynote Lecture 6 Prof. Hans Theliander	L9 Flocculation for Separation Enhancement	G8 Mist and Droplet Separation	M4 Cross Flow Techniques		
14:15 – 14:45	Coffee Break – Fair					
14:45 – 16:00	L10 Poster Session	L11 Filter Aids and Precoat Filtration	G9 Poster Session I	G10 Poster Session II	M5/F5 Poster Session	
16:00 – 17:15	Poster Viewing	L12 Cake Filtration of Slurries with poor Filterability	Poster Viewing	Poster Viewing	Poster Viewing	
	Coffee Break – Fair					

Thursday, 26.02.2015

09:00 – 10:15	F1 Surface Modification of Filter Media	L13 Filter Media	G11 Air Filters – HEPA	M6 Separation of Bio-Products		
10:15 – 10:45	Coffee Break – Fair					
10:45 – 12:00	F2 Production Technology of Filter Media	L14 Sorting and Classification	G12 Air Filters – HVAC	M7 Mechanisms, Models, Simulation		
12:00 – 13:00	Lunch – Fair					
13:00 – 14:15	F3 Fine Fiber and Membrane Manufacturing	L15 Depth Filtration	G13 Industrial Gas Cleaning I	M8 Process and Waste Water Treatment		
14:15 – 14:45	Coffee Break – Fair					
14:45 – 16:00	F4 Numeric Simulation of Porous Structures	L16 Coalescer/Liquid – Liquid Separation	G14 Industrial Gas Cleaning II	M9 Ceramic Membrane Applications		
	Coffee Break – Fair					

Tuesday, February 24, 2015

Plenary Lecture

10:45 - 12:00 h

PL

How could Integrated science change the separation technology in the future?

Dr. Karsten Keller
DuPont, USA

Keynote Lecture 1

13:00 - 14:15 h

K1

Sugar purification from enzymatic hydrolysis products using membrane diafiltration

Prof. Kuo-Jen Hwang, Tamkang University, Taiwan

Dispersion Separation Analysis

13:00 - 14:15 h

L1

Introducing LUMiReader® X-Ray - A new instrument for the evaluation of separation behaviour of concentrated nontransparent dispersions D. Lerche*, D. Kavianpour, A. Zierau, T. Sobisch, LUM GmbH, Germany

Characterization of the separation and segregation behaviour of model paper dispersions, D. Kavianpour*, T. Sobisch, A. Zierau, D.Lerche, LUM GmbH, Germany

Use of photocentrifuge for membrane separation and characterization of solutions filterability, M. Loginov*, N. Lebovka, E. Vorobiev, University of Technology of Compiègne, France

Cake Filtration Analysis

13:00-14:15 h

L2

Wall effect of solid liquid filter test on filter up-scaling, R. Giner, G. Kramer*, Andritz AG, Austria

Systematical laboratory tests with a bucket centrifuge and a pressure nutsche – Comparison of the cake permeability and consequences for the scale-up of batch filtering centrifuges, R. Ebert, E. Verdurand*, M. Schmid, DSM-Nutritional Products, Switzerland; I. Nicolaou, NIKIFOS Ltd., Cyprus

Efficient internal filtration system for solid-liquid separation, M. A. Khodaghali*, A. K. Forsat, Research Institute of Petroleum Industry; M. R. Hemmati Mahmodi, Sorosh Energy Pouya, Iran

Surface Filtration I

13:00 - 14:15 h

G1

Influence of leaks on the overall emission behaviour of bag house filters, O. Kurtz*, J. Meyer, G. Kasper, Karlsruhe Institute of Technology, Germany

Airborne nanoparticle filtration by filter cakes on pulse-jet cleaned filter media, H. Förster*, C. Funk, W. Peukert, University Erlangen-Nuremberg, Germany

Study and characterization of the emitted particles in pulse jet filtration, A. K. Choudhary*, A. Mukhopadhyay, Jalandhar Institute of Technology, India

Gaseous, Liquid, Solid Contaminants

13:00 - 14:15 h

G2

Gas phase adsorption of dimethyl sulfide on activated carbon cloth (GDSEL651), N. Hoda*, A. Topuz, F. Mert, L. Budama, E. Eroglu, Akdeniz University, Turkey

Filtration performance in air-oil separation, I. Parker*, Ahlstrom Filtration LLC, USA; H. Lin, G. Costa, Ahlstrom Italy s.p.a., Italy

New media generation for cabin air filter application, A. Scope, D. Keerl*, MANN+HUMMEL Innenraumfilter GmbH & Co. KG, Germany

Keynote Lecture 2

14:45 - 16:00 h

K2

Selective recovery of valuable plant and biomass compounds through biological membranes exposed to pulsed electric field: A new way for "green" filtration and purification technologies Prof. Eugène Vorobiev, University of Compiègne, France

Decanter Centrifuges and Hydrocyclones

14:45 - 16:00 h

L3

Design of decanter centrifuges – development of laboratory test methods and calculations for separation efficiency prediction, M. Böhlmann, Siebtechnik GmbH, Germany

Hydrocyclone - Design & optimization - A new user friendly and reliable approach, I. Nicolaou*, NIKIFOS Ltd, Cyprus

Experimental and simulation of a novel hydrocyclone - Tubular membrane as overflow pipe, C. C. Wang, R.-M. Wu*, Tamkang University, Taiwan

Cake Filtration Washing

14:45 - 16:00 h

L4

The influence of wetting on washing and filtration properties, M. Burisch*, U.A. Peuker, Technical University Bergakademie Freiberg, Germany

Chemical effects in filtration and washing of blast furnace slag, R. Salmimies*, A. Häkkinen, Lappeenranta University of Technology, Finland; M. Burisch, U.A. Peuker, Technical University Bergakademie Freiberg, Germany

Cleaning of filter media contaminated with yeast by pulsed jets, B. Bollwein*, D. Ulmen, J. Tippmann, T. Becker, Technical University Munich, Germany

Surface Filtration II

14:45 - 16:00 h

G3

Filter movement during pressure pulse regeneration – A comparison of flat media and filter bags with regard to cleaning intensity and acceleration, S. Sobich*, J. Meyer, G. Kasper, Karlsruhe Institute of technology, Germany

Effect of fabric type and dust concentration on filtration performance, A. Mukhopadhyay*, S. R. Swain, Jalandhar Institute of Technology, India

Test method for small scale pulse-cleaned package type dust collection system, A. Morishita*, H. Kudou, K. Kitabayashi, S. Katsushima, AMANO Corporation, C. Kanaoka, Kanazawa University, Japan

Automotive Application

14:45 - 16:00 h

G4

Impact of viscous oil impregnation on the performance of motorcycle engine intake air filters, A. K. Maddineni*, S. Chakote, Varroc Polymers Pvt. Ltd., India; H. Sauter, Germany

Micro scale simulation as part of fibrous filter media development processes - From real to virtual media, J. Weber*, A. Kilian, M. Heim, M. J. Lehmann, MANN+HUMMEL GmbH, Germany

Building a refrigerant recovery recycling machine for HFC-134a: From architecture definition to prototype implementation, B. N. Floresca*, Technological University of the Philippines, Philippines



Keynote Lecture 3

16:45 - 18:00 h

K3

Precoat filtration. Insights into a well-established technology that still offers plenty of opportunities Dr. Eberhard Gerdes, JRS Rettenmaier & Söhne, Germany

Filtration Analysis, Apparatus Selection and Design

16:45 - 18:00 h

L5

Cake forming filtration - From the theory based laboratory tests to the reliable selection and optimal design of filter apparatuses, I. Nicolaou*, NIKIFOS Ltd, Cyprus

The filtration calculator: A novel tool for the "daily needs" of people dealing with cake forming filtration, N. Wagner*, F. Tomasko, FLSmidth Wiesbaden GmbH, Germany

Assessment of turbidity meter / Sensor filter combination in beer filtration, H. H. Kleizen, J.B.J. Kleizen, Dutchap BV; G. J. Beune APT BV, Netherlands

Continuous Vacuum and Pressure Cake Filters

16:45 - 18:00 h

L6

Bypass dust processing in the cement manufacturing process - BHS belt filter allow primary fuel substitution rates of up to 100 percent, C. Steinbinder, T. Ochel*, BHS-Sonthofen GmbH, Germany

Combined continuous pressure and press filtration with a HiBar drum filter, E. Ehrfeld*, R. Bott, T. Langeloh, BOKELA GmbH, Germany

Filtration of hot slurries with HiBar filtration, R. Bott*, T. Langeloh, E. Ehrfeld, BOKELA GmbH, Germany



Surface Filtration III

16:45-18:00 h

G5

Evaluation of the efficiency of filtration processes using precoat materials, S. Schiller*, H.-J. Schmid, University of Paderborn; C. Hellmich, Hellmich GmbH & Co. KG, Germany

Investigating reasons for filter bag failure and developing a method to improve its life span, A. Patnaik*, R. D. Anandjiwala, CSIR Materials Science and Manufacturing and Nelson Mandela Metropolitan University, South Africa

Experimental investigations into the effects of ambient humidity on particle-loaded single filter fibers, Q. Zhang*, University of Wuppertal, Germany

New Membranes

16:45-18:00 h

M1

Characterization of microporous hydrophobic membranes used in membrane distillation process, M. Rezaei*, W. M. Samhaber, University Linz, Austria

Porous water repellent silica aerogel membranes for membrane distillation applications, K.-L. Tung, C.-C. Wang, National Taiwan University; Y.-F. Lin, Chung Yuan Christian University, M. S. Huang, Industrial Technology Research Institute, Taiwan

Revolutionary impact of nanotechnology on advanced membranes: Forward osmosis and solvent stable membranes, M. Peyravi, M. Jahanshahi*, Babol University of Technology, Iran

Wednesday, February 25, 2015

Keynote Lecture 4

09:00-10:15 h

K4

Measuring filter cut points and pore size distributions by challenge testing

Dr. Graham Rideal, Whitehouse Scientific, UK

Backwash Filters

09:00-10:15 h

L7

Development of a high gradient magnetic separator for the application in oil filtration, E. Förster*, K. Menzel, H. Nirschl, Karlsruhe Institute of Technology, Germany

Automatic backwash filter for bath purification, W. Watzinger*, Lenzing Technik GmbH, Austria

Iron and manganese treatment of groundwater by means of pre-treatment and an automatic backwash filter, M. Hochedlinger*, P. Stimpfl, E. Hawle Armaturenwerke GmbH, J. Kölbl, Blue Networks e.U., Austria; P. Galambos, L. Kuzma, Hawle Szerelevénygyártó és Forgalmazó Kft., Hungary; P. Sommerauer, H. Haring, HAWLE Armaturen GmbH, Germany

Modelling and Simulation

09:00-10:15 h

G6

CFD simulation of nanofiber-enhanced air filter media, P. Tronville, Politecnico di Torino, Italy; L.L.X. Augusto, A.C.C. Bortolassi, G.C. Lopes, J.A.S. Gonçalves, Federal University of São Carlos, Brazil; R. Rivers, EQS Inc., USA

Simulation of nanoscale particle movement and deposition, A. Stief*, C. Feuchter, Aalen University, Germany; K. Langfeld, University of Plymouth, UK

Numerical simulation of exhaust gas flow and reaction kinetics in the micro porous soot structure of deposited particles in DPFs, M. Bürger*, U. Janoske, University of Wuppertal, Germany

Micro- and Ultrafiltration

09:00-10:15 h

M2

Sintered metal fibre microfiltration of bio-ethanol fermentation broth, Q. Kang*, R. Dewil, Catholic University Leuven, Belgium; J. Baeyens*, T.W. Tan, Beijing University of Chemical Technology, China

Cleaning usability and flux recovery of ultrasound during and after ultrafiltration processing, A. M. Maskooki*, M. H. Shahraki, M. Mohammadi, RIFST Research Institute of Food Science and Technology, Iran

Functional polymers coupled to ultrafiltration membranes to remove and separate anions from aqueous solution, B. L. Rivas*, J. Sánchez, L. Toledo, University of Concepción, Chile

Keynote Lecture 5

10:45-12:00 h

K5

Filtration – A multi-scale and multi-physics challenge for Simulation

Dr. Martin Lehmann, Mann+Hummel, Germany

Vibration, Magnetic and Electric Enhanced Filtration

10:45-12:00 h

L8

Vibration-enhanced compaction of filter cakes and its influence on shrinkage cracking, S. Illies*, H. Anlauf, H. Nirschl, Karlsruhe Institute of Technology, Germany

Numerical dual-porosity model of solid-liquid expression from electroporated bio-solids, Mahnič-Kalamiza*, E. Vorobiev, University of Technology of Compiègne, France

Optimisation of mineral sludge combined dewatering: Aggregation and constant-current electrofiltration in a filter-press, M. Loginov*, M. Citeau, N. Lebovka, E. Vorobiev, University of Technology of Compiègne, France

Test Systems and Measurements

10:45-12:00 h

G7

Filter media testing in overpressure up to 4 bar – Isobaric detection of fractional efficiency, M. Schmidt*, Palas® GmbH, Germany

The impact of the aerosol generation on the characterization of complete filter or filter media, S. Schütz*, M. Schmidt, Palas® GmbH, Germany

Method and device for inhalation intake assessment of radioactive gas-aerosol mixtures, A. Karev*, A. Tsovianov, Federal Medical Biophysical Center, Russia

Fouling and Scaling

10:45-12:00 h

M3

Ultrafiltration of alginate solutions with ceramic hollow fiber membranes: An experimental study of fouling mechanisms, F. Arndt*, J. Braun, H. Anlauf, H. Nirschl, Karlsruhe Institute of Technology; I. Unger, F. Ehlen, S. Schütz, MANN+HUMMEL GmbH, Germany

Reduction of hollow fiber membrane fouling through electroadsorptive filtration of back wash water, R. Komplenik*, Ahlstrom Filtration LLC; J. Brant, University of Wyoming, USA

The performance of polycarboxylates as inhibitors for CaCO₃-scaling in reverse osmosis-plants, W. Hater, K. Urbahn, A. Icart, ICL Water Solutions; J. Jaworski, N. Kruse, G. Braun*, Cologne University of Applied Sciences, Germany



Keynote Lecture 6

13:00-14:15 h

K6

On local cake properties in liquid filtration

Prof. Hans Theliander, Chalmers University, Sweden

Flocculation for Separation Enhancement

13:00-14:15 h

L9

Speeding up process development by an automated flocculation setup, E. J. Freydel*, M. W. Wilson, S. Beurskens, A.M.C. Janse G. N.M. Ferreira, E.J.A.X. van de Sandt, DSM Biotechnology Center, Netherlands

Implementation of floc characteristics to improve deep bed filtration modelling in water treatment, I. Slavik*, W. Uhl, Technische Universität Dresden, Germany

Approach to determine particle density for modelling purposes in water treatment and supply, I. Slavik*, A. Korrenz, K. Ripl, W. Uhl, Technische Universität Dresden, Germany

Mist and Droplet Separation

13:00-14:15 h

G8

Entrainment of droplets from oil mist filters – Characteristics and relevant parameters, S. Wurster*, J. Meyer, G. Kasper, Karlsruhe Institute of Technology, Germany

Enhanced analysis of droplet separation efficiency of knitted wire meshes by optical particle counter measurements and direct numerical simulation based on tomographies, K. Schmidt*, F. Haller, A. Hellmann, S. Ripberger, Technical University of Kaiserslautern; W. Heikamp, Rhodius GmbH, Germany

Isothermal and isobaric measurements of engine crankcase ventilation filters, S. Schütz, L. Mölter, M. Schmidt, Palas® GmbH, Germany



Cross Flow Techniques

13:00-14:15 h

M4

Separation of catalysts with dynamic precoat filtration on the DYNO filter, E. Ehrfeld*, R. Bott, T. Langeloh, BOKELA GmbH, Germany

Optimization of yield when processing beverages with the dynamic cross flow filter, G. Grim*, Andritz KMPT GmbH

Effect of disk structure on the performance of rotating-disk microfiltration of microalgae, K.-Y. Hwang, S.-E. Wu, Tamkang University, Taiwan

Poster Session I

14:45-16:00 h

L10

Strategies and tools available to solid-liquid separations consultants in industry, S. Wolff*, E. I. DuPont de Nemours, USA

Functionalized filter media for continuous vacuum filtration without vacuum and filtrate pumps, H. Anlauf*, Karlsruhe Institute of Technology, Germany

Cake filtration simulation for poly-dispersed spherical particles, O. Iliev, R. Kirsch, S. Osterroth*, Fraunhofer Institute for Industrial Mathematics, Germany

Analysis of stepwise expression of sake fermentation broth, R. Fukuyama*, A. N. Ginting, T. Tanaka, M. Iwata, Osaka Prefecture University, N. Yabuta, YABUTA Industries, Co., Ltd, Japan; M. S. Jami, Islamic University Malaysia, Malaysia

Groundwater filtration through chalcidonite sand, J. Je -Walkowiak*, Poznan University of Technology, Poland

Application of Iranian zeolite (Semnan area) for removal of environmental pollution of sulfide, S. Karimi, A. Azadmehr*, Amirkabir University of Technology, Iran

Kinetics and thermodynamic adsorption studies of the humic acid adsorption from peat water using Fe₃O₄ nano particles, M. A. Zulfikar*, S. A. Purba, I. Suri, H. Setiyanto, Bandung Institute of Technology, Indonesia

Increasing the filtration rate of new valley phosphate concentrate with cost-effective organic additives, E.A. Abdel-Aal*, Central Metallurgical R&D Institute; E.A. Abdel Rahman, Egypt Phosphate Company; A.T. Kandil, Helwan University, Egypt

Patent-Overview: Wet filtration techniques using non-woven textile fabrics, L. Sinowzik*, Sächsisches Textilforschungsinstitut e.V. (STFI), Germany

Reduction of greywater pollutants using modified hydraulic structure case study: Multi – layer cascade weir, D.W. Abbood*, E. A.Jasim, Mustansiriyia University, Iran

Prospects of use of the Flomin EM-230 additive in the filtering process of the phosphoric slurry A.L. Guimarães, R. F. Pires*, Federal University of Triângulo Mineiro, Brazil

Filter Aids and Precoat Filtration

14:45-16:00 h

L11

Improving filter-aid filtration by means of a new mechanistic process model, M. Kuhn*, H. Briesen, Technical University Munich, Germany

Viscose speciality fibres as filter auxiliaries, P. Wimmer*, R. Scholz, D. Bauer, T. Kandler, Kelheim Fibres GmbH, Germany

Method of comparison for hydraulic filter media, A. Willis*, Hollingsworth & Vose Co. Ltd., UK

Poster Session I

14:45-16:00 h

G9

The performance simulation analysis and experimental research on the air filter of engineering vehicle in highland environment, J.-J. Lu*, Y. Sun, J.-D. Wang, M.-H. Li, J.-X. Li, M.-H. Qiao, North Vehicle Research Institute, China

Characterization of dustiness – Influence of low pressure, T. Londershausen*, E. Schmidt, University of Wuppertal, S. Sander, U. Fritsching, University of Bremen, Germany

Liquid bridge force between two unequal-sized spheres – Problems with mechanical models using a circular bridge shape approach, F. Schröter*, E. Schmidt, University of Wuppertal, Germany

Measurement of the adhesion moment of a particle-wall contact and comparison to simulated values, A. Haarmann*, E. Schmidt, University of Wuppertal, Germany

Determination of the adhesion force between particle and filter membrane using a centrifuge technique A.F. Almeida, M. L. Aguiar*, Federal University of São Carlos, Brazil

Effect of the vibration on deposition of particles during gas filtration using fabric filters, A. M. M. Arouca, F. O. Arouca*, L. G. M. Vieira, J.J. R. Damasceno, Federal University of Uberlândia, Brazil

Simulation of particle-particle & particle-fiber adhesion using star CCM+ from CD-Adapco, L.L.X. Augusto*, G.H. Justi, M.L. Aguiar, V.G.G. Béttega, J.A.S. Gonçalves, G. C. Lopes, Federal University of São Carlos, Brazil

Vertical liquid distribution in filter cartridge during gas-liquid filtration, Z. Liu*, Y. Z. Dang, Z. L. Ji, M. J. Yu, China University of Petroleum, China

Combined separation of ultrafine dust particle and gaseous pollutants emitted by biomass combustions, F. Prill*, S. Schiller, H.-J. Schmid, University of Paderborn, Germany

Numerical simulation of geometry influence on electrostatic precipitators, S. Sander*, U. Fritsching, University of Bremen, T. Londershausen, E. Schmidt, University of Wuppertal, Germany

Reduction of fine dust-emissions at inner city areas – opportunities and limitations of electrostatic precipitators, M. Kaul*, E. Schmidt, University of Wuppertal, Germany

Poster Session II

14:45-16:00 h

G10

The influence of the layout of fabric filter in flow mass filtrate, T. W. C. Pereira, F. B. Marques, F. A. R. Pereira, D. C. Ribeiro, S. M. S. Rocha*, Federal University of Espírito Santo, Brazil

Evaluation of the performance of fibrous filter used with pulse jet cleaning in industrial chemistry, S. S. R. Cirqueira*, F. M. Oliveira, M. L. Aguiar, Fed. University of São Carlos; E. H. Tanabe, Federal University of Santa Maria, Brazil

Study of the electrostatic effect in cement particles in bag filters, F. M. Oliveira, S. S.R. Cirqueira*, M. L. Aguiar, Federal University of São Carlos, Brazil

Quantification of bioaerosols from filtration of real indoor environment, P. F. Rosa*, A. Bernado, M. L. Aguiar, Federal University of São Carlos, Brazil

Evaluate the efficiency of different filter media in removing nanoparticles, A. C. C. Bortolassi*, V. G. Guerra, M. L. Aguiar, Federal University of São Carlos, Brazil

Cut size control of novel gas cyclone separator with sintered metal cone by clean-air injection, K. Fukui*, K. Jikihara, S. Sunada, H. Yoshida, Hiroshima University, Japan

Characterization and performance of different fibrous filters media for collecting nanoparticle, A. C. C. Bortolassi*, V. G. Guerra, M. L. Aguiar, Federal University of São Carlos, Brazil

Degradation of PPS filter media by NOx at high temperature, M. Wada*, H. Wakamatsu, C. Kanaoka, Ishikawa University, Japan

Performance of cellulose filter media in the filtration of gases at high pressures, B. A. Lima, G. C. Lopes, M. L. Aguiar*, Federal University of São Carlos; E. H. Tanabe, Federal University of Santa Maria, Brazil

Separation of particles out of air by botanical collectors, G. Reznik, E. Schmidt*, University of Wuppertal, Germany



Poster Session

14:45-16:00 h

M5

Degradation of ion exchange membranes used for pickling acid regeneration, M. Sartor*, J. Willemsen, T. Reichardt, VDEh-Betriebsforschungsinstitut GmbH; F. Rögner, Cologne University of Applied Sciences, Germany; K. Jacobson, Swerea KIMAB, Sweden

Performance improvement of countercurrent-flow seawater desalination systems in hollow-fiber direct contact membrane distillation modules, C.-D. Ho*, T.-J. Yang, L. Chen, Tamkang University, Taiwan



Dehumidifying air with ion-exchange membranes, I. Ladizhensky, E. Korin, E. Korngold, Ben-Gurion University of the Negev, Israel

Application areas of SARATECH® PBSAC in dialysis techniques, A. Stephan, J. Raiser*, Blücher GmbH, Germany

Multiscale modeling of gas molecules penetration through multilayer graphene membrane, S. Gusarov*, K. Bosnick, National Institute for Nanotechnology, Canada

Poster Session

14:45-16:00 h

F5

Efficient simulations of poroelastic deformations in pleated filters, D. Iliev*, O. Iliev, R. Kirsch, Fraunhofer ITWM, Germany; A. Mikeli, University Lyon 1, France; G. Printzypar, V. Calo, King Abdullah University, Saudi Arabia

Designing advanced filtration media through metal additive manufacturing, N. Burns*, M. Burns, D. Travis, L. Geekie, Croft Additive Manufacturing; A. E. W. Rennie, University of Lancaster, UK

Woven wire meshes - Their characteristics and selection criteria, M. Knefel*, GKD Gebr. Kufferath AG, Germany

Pore size characteristics of nonwoven filters under compression loading, A. Rawal*, Indian Institute of Technology Delhi, India

Cake Filtration of Slurries with poor Filterability 16:00-17:15 h

L12

HiBar steam pressure filtration of coal ultrafines and iron ore concentrates - New developments and results, R. Bott*, T. Langeloh, BOKELA GmbH, Germany

Compressible suspension characterisation and plate-and-frame filter prediction, A. D. Stickland*, E. H. Irvin, S. J. Skinner, P. J. Scales, University of Melbourne; A. Hawkey, Billfinger Water Technologies, Australia; F. Kaswalder, Billfinger Water Technologies, Italy

Dewatering of slurry with poor filterability in basket centrifuge: Discharge of supernatant using bypass filter medium, A. N. Ginting*, R. Fukuyama, T. Tanaka, M. Iwata, Osaka Prefecture University, Japan; M. S. Jami, Islamic University Malaysia, Malaysia

Thursday, February 26, 2015

Surface Modification of Filter Media

09:00-10:15 h

F1

PFOA- and PFOS-free super water- and oil-repellent low pressure plasma nanocoatings for filtration and separation applications, E. Rogge*, F. Legein, Europlasma NV, Belgium

Industrial water and oil repellent nano-coatings for filtration applications, N. Rimmer*, P2i Ltd, UK

Celanese engineered materials for porous filter media, I. Idiyatullina*, Celanese, Germany

Filter Media

09:00-10:15 h

L13

Filter media performance and its influence on filtration results – Experience, expectations and possibilities in vacuum and pressure filtration, A. Seitz*, D. Bartholdi, I. Erlenmaier, C. Maurer, Sefar AG, Switzerland

New developments in high performance woven wire filtration media, M. TheiB*, F. Meyer, F. Edelmeier, Haver & Boecker OHG, Germany

Optimal gradient hydraulic media to maximize dust holding capacity, M. Silian*, S. Jaganathan, Hollingsworth & Vose Co., USA

Air Filters – HEPA

09:00-10:15 h

G11

In-situ efficiency measurement for HEPA-filter, C. Schweinheim*, Caverion Deutschland GmbH, Germany

Modern PTFE membrane filters require appropriate testing methods, R. Bharadwaj*, H. Daruwala, AAF International, USA

An investigation on the shorter lifetime of pleated filter compared to flat sheet, L. Cheng*, J. Becker, A. Wiegmann, Math2Market GmbH; R. Kirsch, Fraunhofer Institute for Industrial Mathematics, Germany



Separation of Bio-Products

09:00-10:15 h

M6

Membranes or molecular sieves in preparing fuel-grade bio-ethanol, Q. Kang*, J. Baeyens, R. Dewil, Catholic University Leuven, Belgium; W. Kong, T. Tan, Beijing University of Chemical Technology, China

Long term experiment for the separation of "green" hydrogen from biomass gasification by a polymer membrane, D. Konlechner*, M. Harasek, H. Hofbauer, Vienna University of Technology, Austria; M. Hackel, AIR LIQUIDE, Germany; E. Sanders, AIR LIQUIDE, USA; K. Bosch, Energie Burgenland AG, Austria

Production Technology of Filter Media

10:45-12:00 h

F2

A neat solution – Modern filters cut with laser technology, F. Matschke, eurolaser GmbH, Germany

Why AOI improves the quality of filter base material and coatings and reduces production costs, H. Oerley*, Dr. Schenk GmbH, Germany

Reel to reel UV lithography for Filter and Screen applications, M. Lehmann*, micrometal GmbH, Germany

Sorting and Classification

10:45-12:00 h

L14

Electromagnetic separation (EMS) of high-temperature superconductor, E. Broide*, Hebrew University, Israel

Optimization of semi-continuous centrifugal classification processes for colloidal products, M. Konrath*, H. Nirschl, Karlsruhe Institute of Technology, Germany

Physical separation and disposal of secondary waste from the decommissioning of nuclear facilities, M. Brandauer*, S. Gentes, S. Stiefel, M. Haist, Karlsruhe Institute of Technology; J. Starflinger, Institute of Nuclear Technology and Energy Systems, Germany

Air Filters – HVAC

10:45-12:00 h

G12

Reducing energy consumption through advances in mechanical Ashrae air filtration media, C. Desquilles*, P. Blanckaert, Lydall Performance Materials SAS, France; D. Sullivan, G. Crosby, Lydall Performance Materials, USA

Saving cost with novel filter media solutions for indoor air quality, I. Parker*, Ahlstrom Filtration LLC, USA

How regulatory changes drive innovation in synthetic filter media for pocket filters, A. Boni, B. Keil*, Hollingsworth & Vose, Germany

Mechanisms, Models, Simulation

10:45-12:00 h

M7

Filtration of finest nanoparticles < 15 nm from liquids - A quantitative study, D. Segets*, W. Peukert, University Erlangen-Nuremberg, Germany; S.-C. Chen, T. Y. Ling, D. Y. H. Pui, University of Minnesota, USA

Use of computational fluid dynamics (CFD) for the design of apparatuses for cross flow filtration, J. Barth*, S. Ripperger, University of Kaiserslautern, Germany

Simulation of osmotic and reactive effects in membranes with resolved microstructure, O. Iliev, K. Leonard, Fraunhofer Institute for Industrial Mathematics, Z. Lakdawala, DHI-WASY GmbH, Germany; E. di Nicolò, Solvay Specialty Polymers, Italy; V. M. Calo, G. Printzypar*, King Abdullah University, Saudi Arabia

Fine Fiber and Membrane Manufacturing

13:00-14:15 h

F3

High flux solvent resistant nanofiltration membranes from interfacial polymerization, S.-P. Sun, T.-S. Chung, National University of Singapore, Singapore

Molecular orientation in highly stretched ePTFE filtermedia, K. J. Choi, Clean & Science Co., Ltd., USA

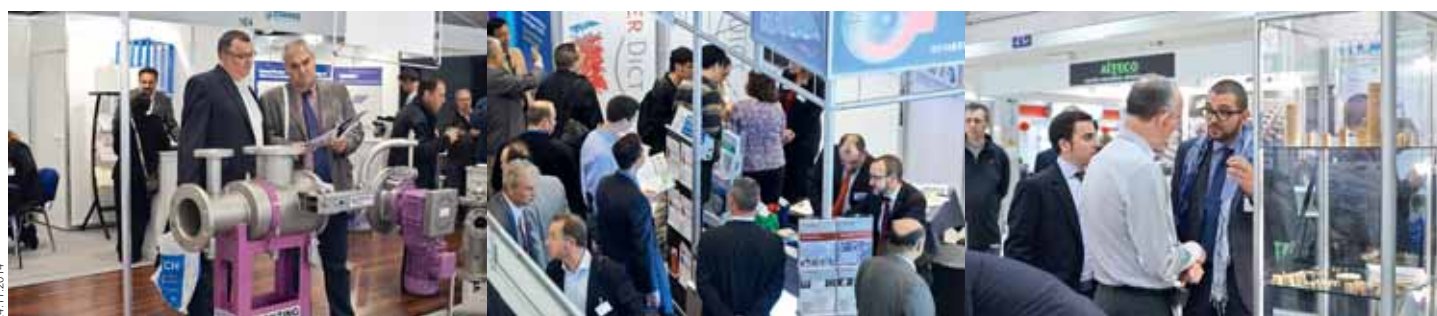
Cost-effective production of track-etched UF membranes, S. Makkonen-Craig*, M. Paronen, Arcada University of Applied Sciences, Finland

Depth Filtration

13:00-14:15 h

L15

MNMs: a model for the simulation of depth filtration of non-Newtonian suspensions in granular media, R. Sethi*, T. Tosco, C. Bianco, Politecnico di Torino, Italy



Experimental study and numerical simulation of the flow-induced deformation of filtering media in automotive transmission filters, M. Kabel, R. Kirsch*, S. Staub, Fraunhofer Institute for Industrial Mathematics, Germany, D. Bernards, M. Dederich, IBS FILTRAN GmbH, Germany

Investigation of depth filtration of aqueous suspensions with particles greater than 1 micron, L. Petersen*, S. Ripperger, Technical University of Kaiserslautern, Germany

Industrial Gas Cleaning I

13:00-14:15 h

G13

Separating dust out of process air flow using drum filters, H. Sauter*, F. Engel, LTG Aktiengesellschaft; U. Schneider, Gebr. Röders AG, Germany

Design of vacuum cleaned dust filter, T. Laminger*, J. Wolfslehner, W. Höflinger, Vienna University of Technology, Austria

Gas phase advanced oxidation cleans industrial pollution and smell, C. Meusinger*, M. S. Johnson, University of Copenhagen; T. Rosenørn, INFUSER A/S, Denmark; F. Hartung, INFUSER Deutschland GmbH, Germany

Process and Waste Water Treatment

13:00-14:15 h

M8

Advanced wastewater treatment with ultrafiltration, L. Causemann; S. Krause*, University of Applied Science Darmstadt, Germany

Small scale plants for resource efficiency training in the Indian metal industry, M. Sartor, P. Ivashechkin, VDEh-Betriebsforschungsinstitut GmbH; F. Rögner*, Cologne University of Applied Sciences, M. Enders, Simatech GmbH, Germany; M. Balakrishnan, TERI University, India; T. Schneiker, Scanacon AB, Sweden

A 3,000m³/day tubular membrane Ffilter (TMF™) system installed in Korea for wafer backgrinding water reclamation, D. Frick*, POREX Filtration, USA; S. Yang, POREX Filtration, China

Numeric Simulation of Porous Structures

14:45-16:00 h

F4

Methods of filter media pore space analysis based on geometrical characteristics, G. Bälz*, R. Handel, B. Renz, A. Enderich, Mahle Filtersysteme GmbH; C. Feuchter, Aalen University, Germany

Simulation of cake filtration for polydisperse particles, J. Becker*, L. Cheng, A. Wiegmann, Math2Market GmbH, Germany

Automatic fiber thickness measurement in SEM images validated using synthetic data, P. Easwaran*, O. Wirjadi, T. Prill, Fraunhofer Institute for Industrial Mathematics, M. Lehmann, 2MANN+HUMMEL GmbH, S. Didas, University of Applied Science Trier; C. Redenbach, Technical University of Kaiserslautern, Germany

Coalescer/Liquid-Liquid Separation

14:45-16:00 h

L16

Oily and wastewater separation by electroflotation, I. L. Nascimento, E. Mattedi, M. F. Cometi, W. V. Paiva, S. M. S. Rocha*, Federal University of Espirito Santo; E. R. Nucci, Federal University of São João Del Rei, Brazil

Preliminary studies of new water removal element in purification applications of diesel fuels and lube oils, R. Chen*, Kaydon Filtration Corp., USA

Challenges of testing fuel water separation efficiency, G. Venkateswaran, A. Goodyby*, Ahlstrom Transportation Filtration, USA

Industrial Gas Cleaning II

14:45-16:00 h

G14

Bag Filters: DURAtes microfiber felt for high-efficiency filtration, D. De Angelis*, E. Galletta, L. Cattaneo, L. Balzaretto, Testori S.p.A., Italy

Pressure resistance parameters and dedusting performance of differently sized needle felt bags in a pilot scale test facility, F. Seffrin*, D. Hess, Balcke-Dürr GmbH, Germany

Intelligent filter solutions with focus on low weight/foot print and premanufactured design, L. Gamborg*, M. Staben, L. Korkholm, K. Poulsen, B. O. Andersen, FLSmidth A/S, Denmark

Ceramic Membrane Applications

14:45-16:00 h

M9

Ceramic hollow fiber membranes as new filter media and their application in oil/water separation processes, S. Schütz*, F. Ehlen, I. Unger, MANN+HUMMEL GmbH; M. Ebrahimi, S. Kerker, P. Czermak, University of Applied Sciences Mittelhessen, Germany

Investigation the performance of cross-flow micro-filtration of titanium dioxide suspension, T. H. T. Trinh, W. Samhaber, University Linz, Austria

Hybrid flotation-filtration process for oil water separation based on ceramic membranes, M. Beery*, J. Ludwig, L. León, akvolution GmbH, Germany

Please note that the Programme is subject to amendments.

24.11.2014

The Conference Registration includes

Congress Proceedings featuring all papers in an abstract book and full paper versions on USB stick

Refreshments during breaks

Lunch/es

Welcome Reception on 24 February, 2015

Entrance to the FILTECH 2015 Exhibition from 24-26.02.2015

FILTECH 2015 Exhibition Catalogue

Cologne Public Transport Ticket

Fees already include German VAT.

Register online: <https://filtech.de/registration2015/>

CFD SIMULATION OF NANOFIBER-ENHANCED AIR FILTER MEDIA

Paolo Tronville*, Politecnico di Torino, Corso degli Abruzzi 24, 10129 Torino - Italy;
 L.L.X. Augusto, A.C.C. Bortolassi, G.C Lopes, J.A.S Gonçalves,
 Universidade Federal de São Carlos, São Carlos, Brazil;
 R.D. Rivers, EQS Inc., Louisville, Kentucky 40204 USA

ABSTRACT

The first step in a CFD analysis of filter media flow is to create a computational domain geometry which imitates the simulated media as closely as is practical. The media in the present study combined a relatively flat web of nanofibers with a cellulosic fiber support media. Fig. 1, a SEM image of the material at 1000x, shows the highly random nature of the two media elements, and the difference in scale between them. Fig. 2 is a 20000x SEM image of the same media, showing the polymeric nanofiber web, and behind it, a single cellulosic fiber having a diameter perhaps 100 times the diameter of the nanofiber web elements. A CFD grid suited to calculating the flow patterns through the cellulosic media structure would be far too coarse to simulate flow around the nanofiber web elements. This scale difference forces some assumption about the interaction between the media layers.

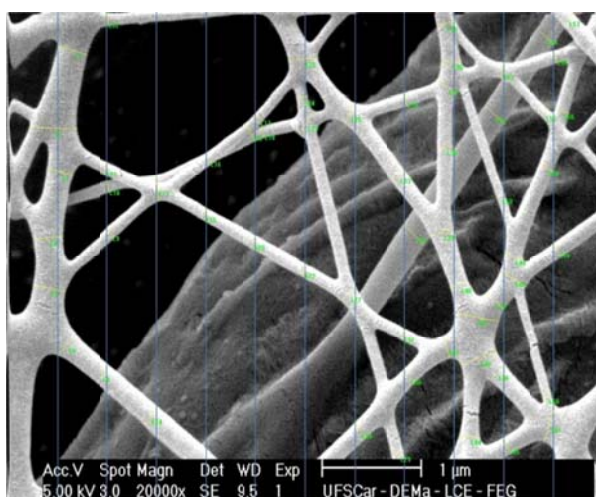


Fig. 1 Nanofiber/cellulosic media, 1000x. Fig. 2. 20000x image, showing nanofiber details.

Our models are limited to two dimensions, representing cross-sections cut through the media in the direction perpendicular to figures 1 and 2. Our initial studies modeled the nanofiber web alone, on the assumption that the flow around the nanofibers is not greatly influenced by the presence of the downstream cellulosic fibers. It is apparent from Fig. 2 that not all parts of the nanofiber web have circular cross-sections. Our image-analysis technique samples the distribution of fiber diameters by scribing parallel lines across the image (faintly visible here). The diameter of the web element at each line/fiber crossing is tabulated. An estimate is made of the maximum width on the image for which the web element cross-section can be considered circular. We make the assumption that the relatively flat web elements linking round sections have oval cross-sections, all of the same thickness. We found that the distribution of web element widths is “doubly-truncated log-normal”, meaning that both lower and upper limits to the widths exist. This geometry was used with a CFD code to calculate particle capture, and compared to results of tests on the actual media.

KEYWORDS

CFD, Nanofiber, Cellulose Fibers, Fiber Size Distribution, Flow simulation

CFD SIMULATION OF NANOFIBER-ENHANCED AIR FILTER MEDIA

Paolo Tronville*, Politecnico di Torino, Corso degli Abruzzi 24, 10129 Torino - Italy;
 L.L.X. Augusto, A.C.C. Bortolassi, G.C Lopes, J.A.S Gonçalves,
 Universidade Federal de São Carlos, São Carlos, Brazil;
 R.D. Rivers, EQS Inc. Louisville, Kentucky 40204 USA

It has been known for many years that fine fibers contribute greatly to the particle-capture efficiency of fibrous air filters (Graham et al., 2002; Podgórski et al., 2006). HEPA and ULPA filter media, for example, contain glass fibers having diameters less than 1 μm . Nanofibers – defined as fibers or fiber-like structures with dimensions less than 100 nm, or 0.1 μm (Rai et al., 2009; Warheit et al., 2008) – have only in recent years been added to air filter media. Simulation of the behavior of media containing nanofibers poses problems and uncertainties that have generally been overcome for media with coarser fibers. Since the addition of nanofibers has been shown to improve particle-capture efficiency adding to media a little pressure drop, it is important to develop simulation techniques which accurately predict the effects of nanofibers.

Air Filter Media Studied

The fibrous filter media described in this study has a rather unique structure. A scanning-electron microscope (SEM) image of the cross-section of this media is shown in Fig. 1.

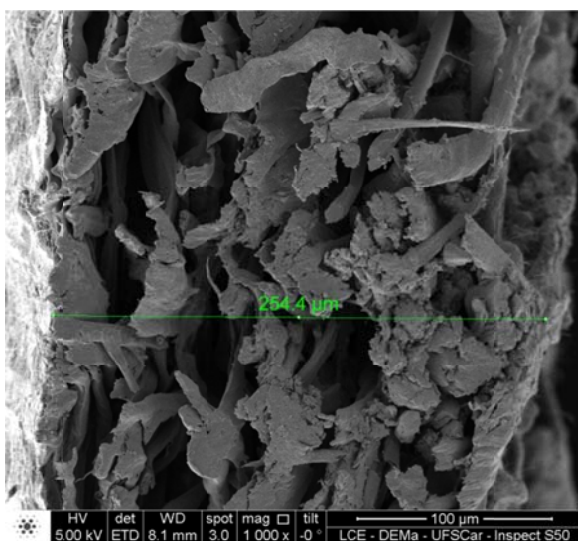


Fig. 1 - NC13 media, cross-section at 1000x. White region at left is nanofiber web, seen at a slight angle.



Fig. 2 - NC13 media, showing nanofiber web applied to upstream face of cellulosic support media (1000x)

The highly irregular grey shapes filling most of the image are cross-sections of the cellulosic support media. Fig. 2 shows the nanofiber web, which covers most of the upstream face of the support media. Fig. 3 is a higher-magnification image (20000x) of a portion of the web. Most of the length of the nanofiber web elements consists of straight sections with apparently round cross-sections. These round sections are joined by relatively flat links, which have rounded edges. The aim of this study was to model these two very different layer structures – nanofiber layer and cellulosic support media – and see how closely CFD simulations of flow through the two could model both the pressure drop across the layers and the particle-capture efficiency of each. This study is incomplete, but we have developed some tools which will assist its completion.

SEM Image Analysis

The first step in any CFD study is to develop a model of the geometry to be simulated. Analysis of SEM images can yield quite accurate simulations of complex geometries. We began with analysis of images like Fig 3. Data from several images were merged, because the area of media shown in each image is an extremely small sample of even a square centimeter of the actual media (Fig. 3 represents about 0.0003 cm^2 of the media). Parallel lines were drawn digitally across the images, and intersections between these lines and the web elements identified. The width of the element images was measured, in a direction normal to the element edge at the intersection.

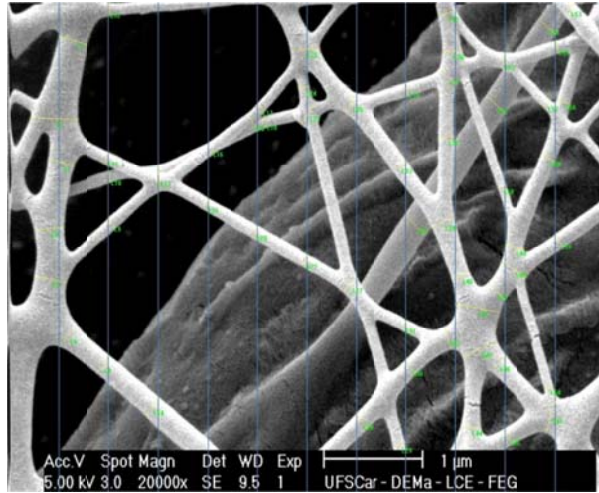


Fig. 3 - NC13 media, detail of nanofiber web

For the straight, round elements this width corresponds to the diameter of the “nanofiber”. The parallel-line scheme effectively integrates the length of “fiber” corresponding to each diameter measured.

The treatment of the links joining round sections is somewhat arbitrary. In fact, the links probably vary in thickness, but this thickness cannot be determined from the image. We therefore made the analysis based on the assumption that all links have the same thickness, and that the link thickness is equal to the largest diameter of a round section observed. For the set of images analyzed, this diameter/thickness was estimated at 341 nm. On this basis, a section cut through the web would look somewhat like Fig. 4.

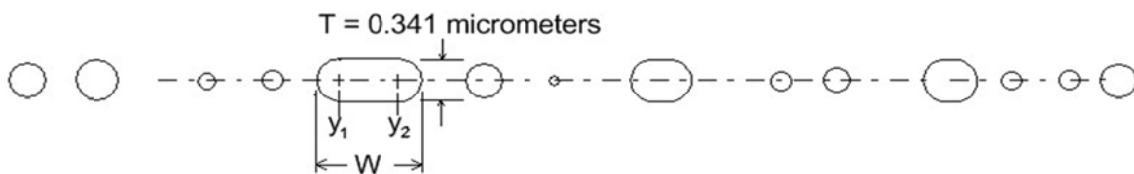


Fig. 4 - Example of nanofiber web cross-section, showing random location of elements, with random diameter circular cross sections, and oval links, all of the same thickness T .

Curve-Fitting the Distributions

The statistics of the width distributions are dependent on the number of line/web intersections, and may be very ragged in the tails of the distributions. It may also be necessary to generate more elements in a CFD domain than were actually identified in the images. For these reasons, we fitted the data to a “truncated-log-normal” distribution. To help

this fitting process, it is useful to plot the measured distribution data on “log-probability” graph paper. The computer program we developed does this. A sample of the display for the nanofiber web data is shown in Fig. 5.

Using the log and probability scales, as in Fig. 5, a truly log-normal distribution plots as a straight line. The distribution shown in Fig. 5 is obviously not truly log-normal. The program allows the user to specify the minimum and maximum sizes that can be expected for the data plotted. The user then selects the end-points of a central portion of the distribution, and chooses whether to fit this portion with a straight line ($Y = A + BX$) or a second-degree polynomial ($Y = A + BX + CX^2$).

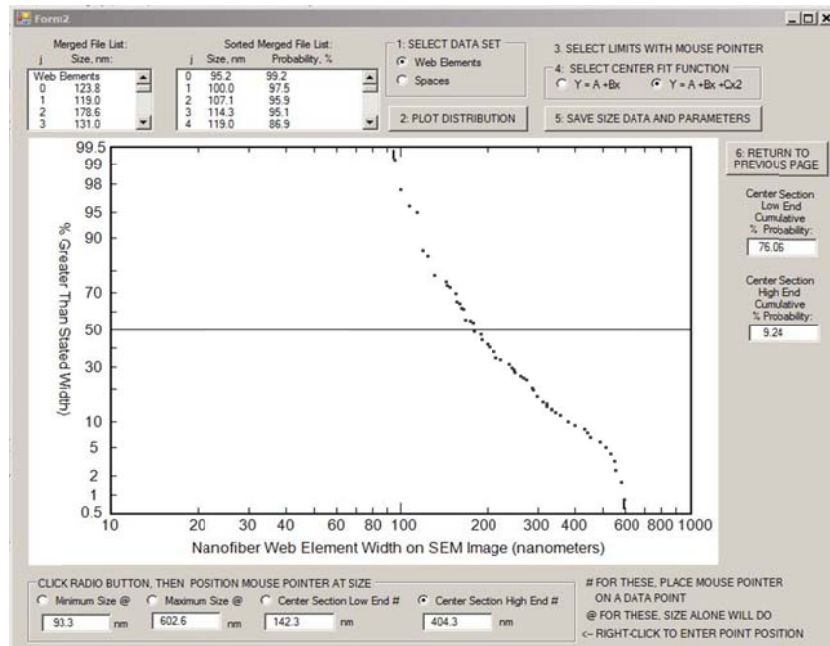


Fig. 5 - Computer display of truncated log-normal distribution (nanofiber web data)

In the case shown, the $Y = A + BX + CX^2$ fit for the center section of the distribution seems warranted. The program then calculates fits to the data in both tails, using a function which is asymptotic to the chosen minimum and maximum values. The fitted function is:

$$Z = G \cdot e^{-K \cdot u} \quad \text{or} \quad \ln(z) = \ln(G) - K \cdot u$$

where z , G , and u are as shown in Fig. 6 for the region between about 90 and 140 nm. The same function is used to fit the points for the upper asymptote, here between 440 and 620 nm.

With the parameters of the curve-fits in hand, the user can generate any required number of shapes matching the distribution, as shown in Fig. 4.

A domain geometry like Fig. 4 requires that the shapes be spaced apart randomly as the fibers and links are in Fig. 3. To accomplish this, we tabulated the lengths of the line segments crossing the spaces between each web element in images like Fig. 3. The distribution of these line segment lengths is also truncated log-normal, and its parameters can be established using the same program as was used to analyze the web elements.

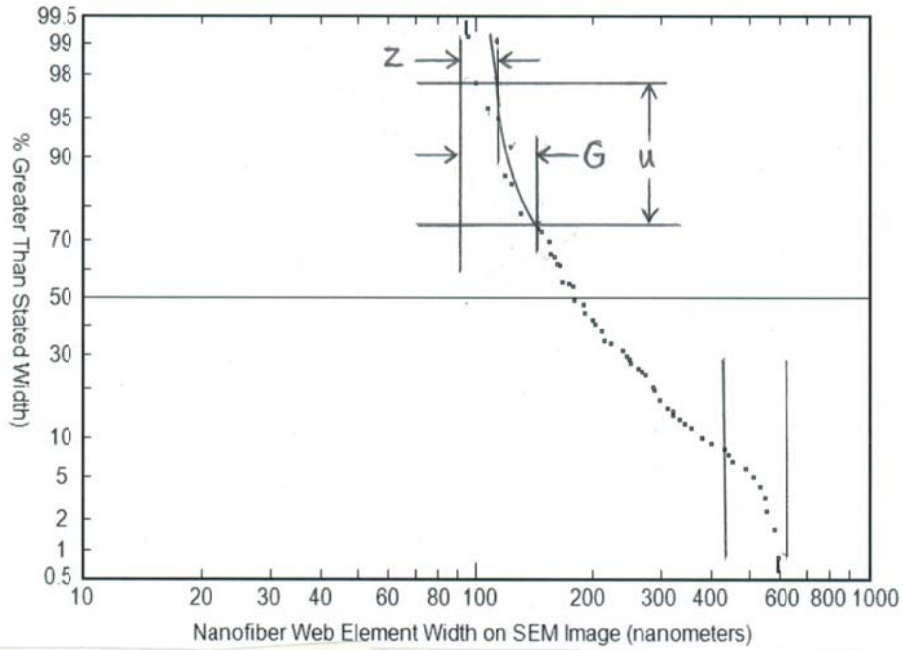


Fig.6 - Curve-fitting to truncated-log-normal distribution: tail asymptotes

Knudsen Length and Slip Boundary Conditions

As the program calculates the sizes and positions of the web elements for the CFD domain, it also determines whether each element is of such size that slip conditions should be applied to its boundaries. The criterion for slip is the Knudsen number of the shape, $Kn = \lambda/L$, where L is a “significant dimension” of the body and λ the mean free path of the molecules in the gas simulated. For a circular cylinder (hence circular fibers), $L = R$, the radius of the cylinder. For non-circular bodies, we define L as:

$$L = 2 \cdot \frac{\text{area of body cross-section}}{\text{perimeter of body cross-section}}$$

The area and perimeter of each oval in our case is easy to calculate from the values of W and T in Fig. 4. In all cases, L thus calculated for all web elements is such that for λ the test air in our laboratories, slip conditions must be applied to simulations of the web. Tronville et al. (2012) described with more details the interaction of gas molecules with fiber surfaces.

Simulation of Cellulosic Media Fibers

Although much of the nanofiber web lies between contacts with the cellulosic support fibers, we cannot assume that the flow through the nanofiber web is entirely independent of the presence of the cellulosic support fibers. Simulating the nanofiber web layer and the complete thickness of the cellulosic media is not practical, because of the large difference in scale of the elements in each layer. We could, however, add simulations of parts of a few cellulosic fibers to the CFD domain, immediately downstream of the nanofiber web, and thus in part model the effect of the support fibers on the nanofiber web flow.

Even for this limited inclusion of the cellulosic support media fibers in the CFD domain, we cannot simply introduce an arbitrary set of shapes of arbitrary size. The solids fraction in the space immediately downstream of the nanofiber web must approximate the solids fraction in the actual media, and also have sizes matching the actual media.

Analysis of SEM images like Fig. 1 provides the necessary information.

The solids fraction of the media is approximated by $\frac{\text{sum of the fiber section areas}}{\text{area of the image rectangle}}$.

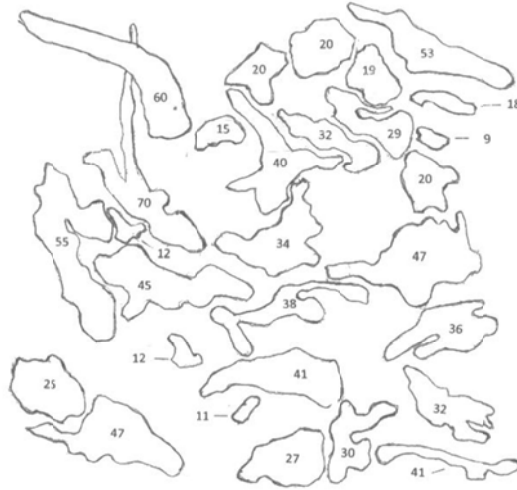


Fig.7 - Outlines of the fiber cross-sections in Fig. 1

Image-analysis software exists that can determine areas of irregular shapes such as those in Fig. 1, or one can weigh a paper print of the image rectangle, then cut the shapes from the print, then weigh the collection of shapes to obtain the relative areas. The “size” of the individual shapes is difficult to define. We define size in this case as the longest distance between two points on the shape perimeter. The numbers on Fig. 7 are the values of these distances (in millimeters) on a paper print of Fig. 1. Not surprisingly, these distances proved to have a truncated log-normal distribution, which could be fitted as described above. The calculated parameters allowed us to generate some shapes to represent the cellulosic fibers immediately downstream of the nanofiber web. The parameters can also be used to create a domain which simulates the geometry of the full depth of the cellulosic media.

Generation of Cellulosic Fiber Shapes and Their Location in the CFD Domain

Fig.1 shows how irregular the cellulosic fiber cross-sections are. We decided that these shapes could be simulated by many-sided polygons, built around some basic general forms: triangles, pentagons, and U-shapes. A program was developed to produce irregular boundaries on the sides of these basic shapes, which were also randomized in both overall size and proportions. Examples of the forms produced are shown in Fig. 8. These shapes are generated within a group of basic shapes – rectangles, triangles, U-shapes – for which the basic sides are replaced with jagged lines made of short line segments. Both the size and the angular orientation of the finished polygons are set to random values by random-number generators. The vertices of the polygons are saved in a file for later positioning in a computational domain.

The 2D shapes in the CFD domain cannot be allowed to overlap, since that would represent two fibers occupying the same space. The test for overlap between circles is simple, but the test for overlapping irregular polygons is not. A naïve approach for overlap tests each line segment in the perimeter of the first shape for intersection with each line segment in the perimeter of the second shape. For the shapes we generate, 30 or more line segments in a shape perimeter are not unusual; at test for overlap of two such shapes could require 900 tests for each potential overlap.

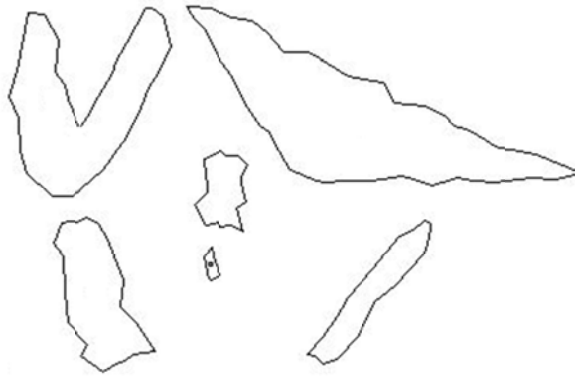


Fig.8 - Examples of irregular polygons simulating the cross-sections of cellulosic fibers

The number of tests is reduced substantially by determining the lowest and highest X- and Y-coordinates of the polygon vertices of each shape. These define a rectangle which circumscribe the shape. If the circumscribing rectangles of two shapes do not overlap, the polygons cannot overlap; if the circumscribing rectangles do overlap, the polygons may overlap, but a much reduced number of polygon sides need to be tested for intersections.

The area of each polygon is needed, for the sum of their areas in the domain must be at least approximately equivalent to the solids fraction of the cellulosic media. The calculation of the exact area of these irregular polygons is very complicated. We chose to allow an approximation of the area to suffice. The procedure for generating the irregular perimeters of the polygons allows a relatively simple calculation of the possible lower and upper limits for the areas of the polygons. The average of these two values is close enough to the exact area of each irregular polygon to use in calculating the fractional solids of the simulated geometry.

CFD Simulations: Nanofiber web Input Geometry and Computational Grid

The CFD domain width (the Y-direction for the geometry) was set at 200 μm to allow a reasonable sample of the nanofiber web elements to be included. An empty zone 1 μm deep (the X-direction) was provided upstream of the nanofiber web, with a uniform entrance velocity set across the domain width. For the initial runs, the X-velocity component $V_{x,0}$ was set at 10.4 cm/s, and the Y-velocity component set at 0. A zone 1 μm deep was also provided downstream of the nanofiber web, with the pressure derivative $\partial P/\partial x$ set equal to 0 along the downstream boundary of this empty zone. A grid was created in the domain with cells made progressively smaller as the nanofiber web element boundaries were approached, to allow resolution of the flow in the nanofiber web space. Longest and Vinchurkar (2007) stated that the grid should be refined in regions of interest to increase the resolution and reduce discretization errors. In the case of this study, the grid was refined near the fibers, which is the region of interest and where the gradients of pressure and velocity are larger. A portion of the grid, 11 μm wide by 2.34 μm deep, is shown in Fig. 9. The complete domain is about 18 times as wide as shown here.

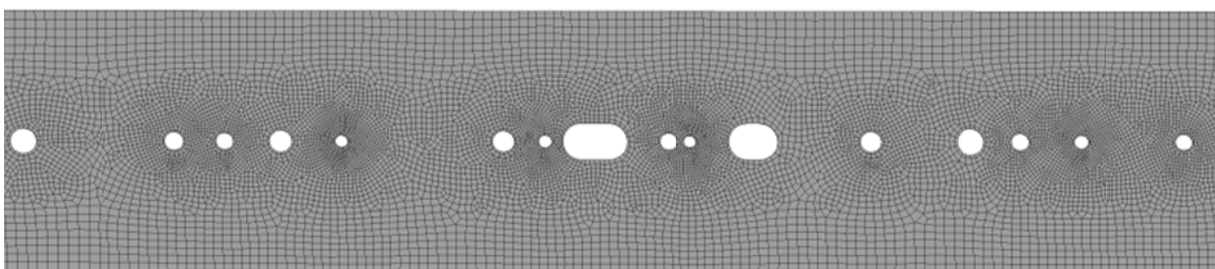


Fig. 9 - Portion of computational grid, showing refinement near web elements

Results of CFD Simulations: Pressure Drop

Runs of the ANSYS Fluent code were made using the geometry described, one with zero-slip at the web element boundaries, and one with full-slip at the boundaries. Fig. 10 shows the pressure patterns which were obtained, using an inlet velocity of 10.4 cm/s. The airflow direction is upward in Fig. 10A and 10B. The surprising thing about these two patterns is how little they differ in appearance. However, there is in fact substantial variation between the average pressure drops across the nanofiber web, depending on the slip level assigned to the nanofiber web boundaries.

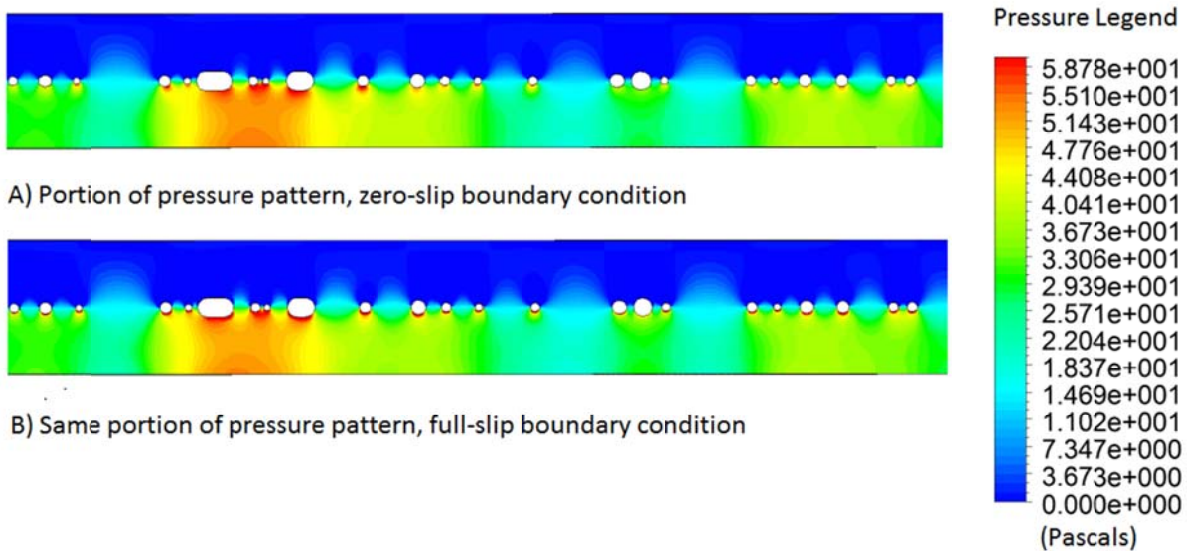


Fig. 10 - Portions of CFD-computed pressure patterns

The pressure drop across the domain in Fig. 10 obviously varies for different values of the Y-coordinate, but one cannot accurately determine from images like Fig. 10 the drop at any Y value. The Fluent code has built-in procedures which simplify the calculation of the average value of pressure drop between two lines with constant X coordinates. For the no-slip case, Fig. 11 shows the pressures along the line 1 μm upstream of the nanofiber web, and Fig. 12 the pressures along the line 1 μm downstream of the nanofiber web. Fluent calculates the average values of pressure along each line. The difference between these two averages is the average pressure drop between the lines, in our case, the pressure drop across the nanofiber web. For the zero-slip case at 10.4 cm/s this was 27 Pa. Fig 13 and Fig.14 show the same pressure variations for the full-slip case; here, the difference was 17 Pa.

Samples of the support media without its nanofiber web layer were not available from the manufacturer, and it is all but impossible to remove the nanofiber web from the cellulosic support. The only pressure-drop measurements that could be made were, therefore, for the composite, two - layer media. The pressure drop across the two layers is essentially additive, so that when we obtain simulations of the full depth of the cellulosic media, the sum of the simulated pressure drops across the two layers can be compared with the measured pressure drop across the actual composite media. An accurate simulation predicts both pressure drop and particle capture efficiency accurately, but particle-capture efficiency is a more sensitive verification of the CFD simulation than pressure drop.

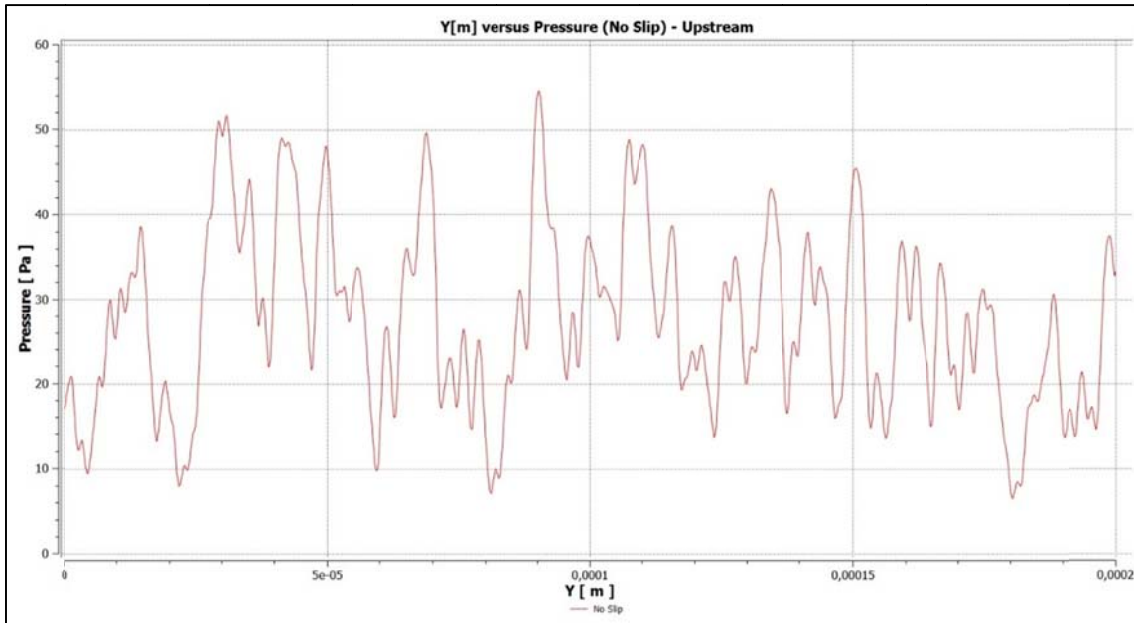


Fig. 11 - Fluent output of pressure along the line 1 μm upstream of the nanofiber web (No-slip case at 10.4 cm/s media face velocity)

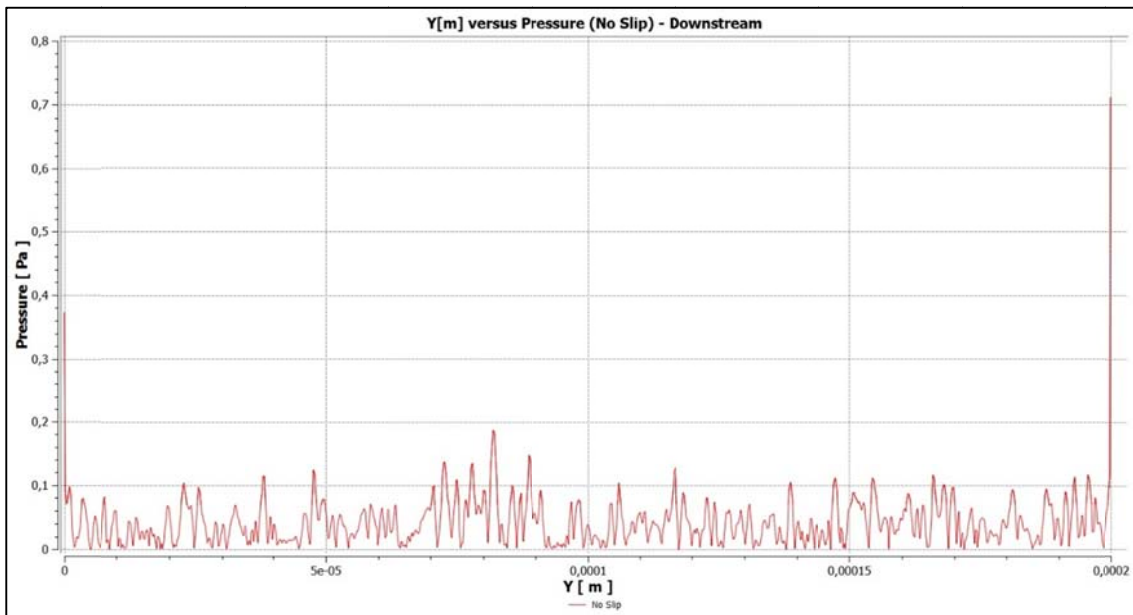


Fig.12 - Fluent output of pressure along the line 1 μm downstream of the nanofiber web (No-slip case at 10.4 cm/s media face velocity)

There is reason to believe that particle capture takes place almost entirely on the nanofiber web, and that the cellulosic media is little more than a means of supporting the nanofiber web. When it is not possible to separate the layers, CFD simulation can quantify the relative contributions of the two layers to particle capture and pressure drop.

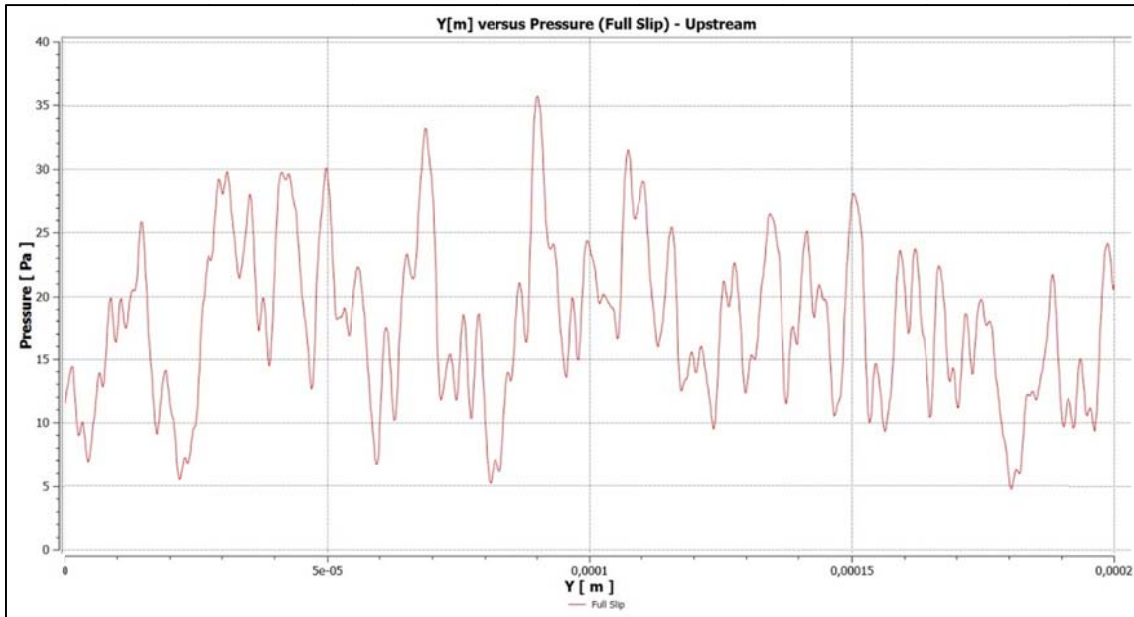


Fig.13 - Fluent output of pressure along the line 1 μm upstream of the nanofiber web (Full-slip case at 10.4 cm/s media face velocity)

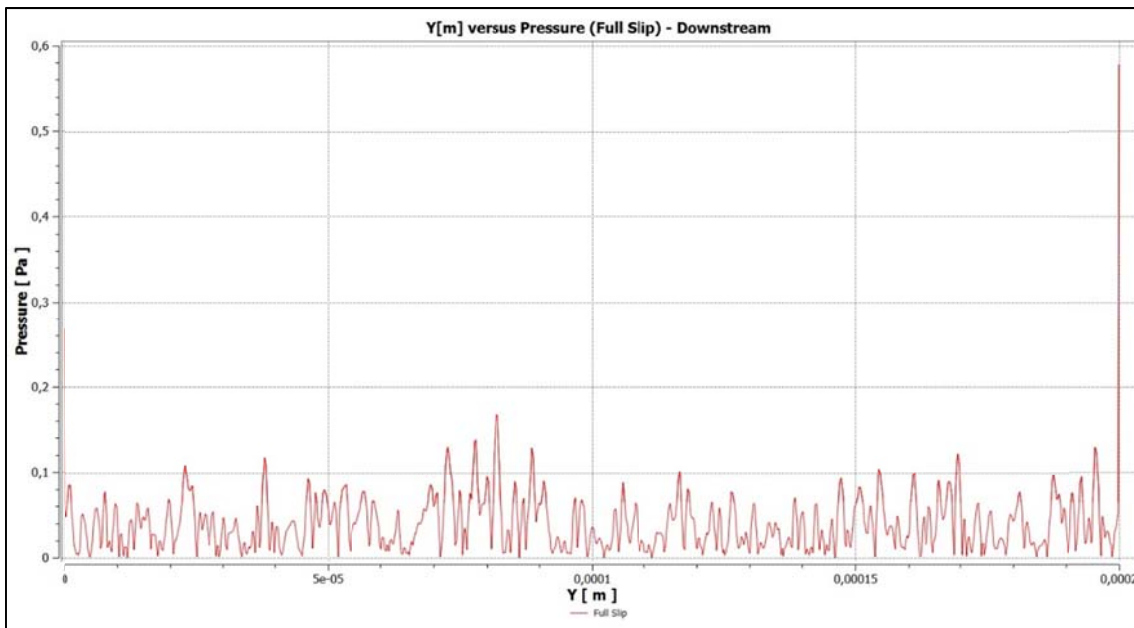


Fig.14 - Fluent output of pressure along the line 1 μm downstream of the nanofiber web (Full-slip case at 10.4 cm/s media face velocity)

We have not yet completed simulations of the cellulosic support media flow, hence cannot compare the measured data for the composite media to simulated values. Table 1 gives the CFD-simulated pressure drops across the nanofiber web alone, for both full-slip and no-slip conditions, and the pressure drop across the composite media. The Knudsen Numbers for all elements of the nanofiber web was high enough that the full-slip column should be correct. The contribution of the nanofiber web layer to overall pressure drop thus appears to be quite small. Wang et al. (2008) investigated filters containing a layer of nanofibers and found values of pressure drop with the same order of magnitude than those found in this work.

Table 1 - Simulated and measured media pressure drops

Media face velocity [cm/s]	Nanofiber web simulated pressure drop [Pa]		Composite media experimental pressure drop [Pa]
	Full Slip	No Slip	
5.2	8.9	13.8	108
6.5	11.1	17.2	131
7.8	13.3	20.6	155
10.4	17.8	27.5	204
13.0	22.2	34.4	258
15.6	26.7	41.3	306
17.3	20.6	45.8	340

Results of CFD Simulations: Velocity Patterns

The CFD code provides displays of the velocity patterns calculated for the domain geometry. Fig. 15 shows the results for the same portion of the domain that is shown in Fig. 10. These patterns show that in the zero-slip condition, velocity is indeed zero around the entire boundary of each simulated web element. The velocity at the exact boundaries cannot be seen at the scale, so that the behavior for full-slip cannot be seen, but it is clearly different from the zero-slip case. The higher velocities through relatively wide openings in the nanofiber web are also apparent, along with the influence of these higher velocities on the flow around nearby web elements.

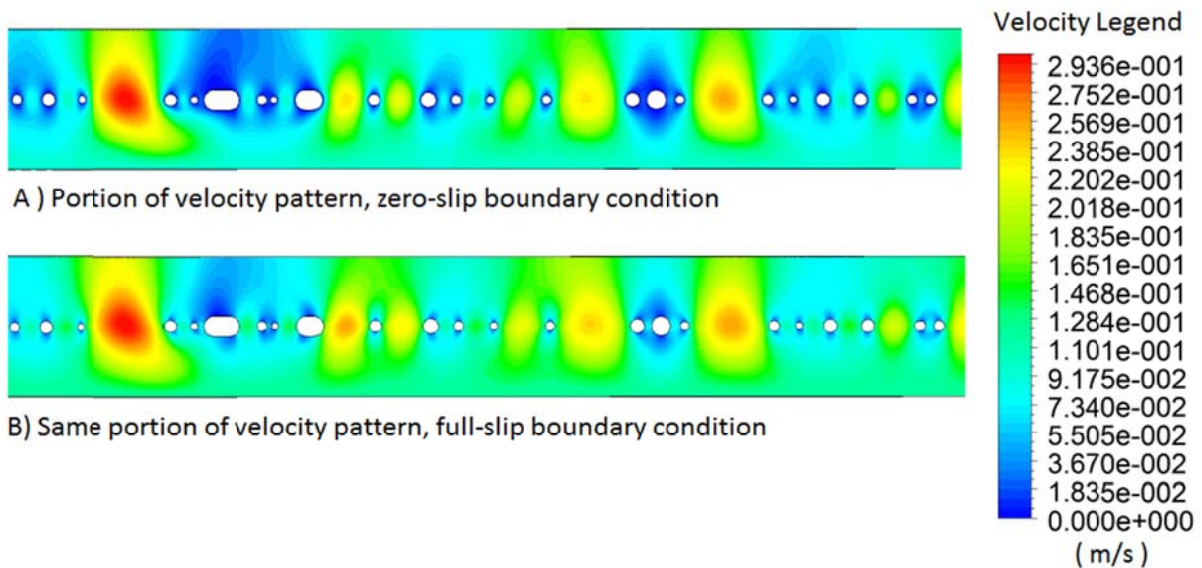


Fig.15 - Portions of computed velocity patterns

Results of CFD Simulations: Particle Capture

A sample of the NC13 media was tested at Politecnico di Torino using a polydisperse DEHS aerosol and a PMS LAS-X II laser light-scattering aerosol particle spectrometer. The media velocity was 10.4 m/s. Table 2 gives the results of that test. We have not yet obtained CFD simulations of particle capture using the domain geometry of Fig. 9, which gave the pressure and velocity patterns of Fig. 10 and Fig. 15.

Table 2 - Penetration Values NC13 Media at 10.4 cm/s, DEHS Aerosol

Diam. [nm]*	110	134	173	224	296	397	520	671	866	1225	1732	2449
Pen. [%]	67.4	72.2	66.5	61.0	53.0	41.0	27.3	18.6	11.7	3.8	1.2	0.6

*Mid-channel diameter, nanometers, PMS LAS-X II aerosol spectrometer

Anticipated Further Research

We will first add simulations of particle capture of the nanofiber web at several media face velocities, comparing the simulations to test values. We will measure the solids fraction of the cellulosic support media, then generate the domain of the cellulosic media using polygon simulations of its fiber cross-sections. CFD runs under zero-slip conditions for the cellulosic media will allow us to compare its pressure drop and particle capture combined with the nanofiber web to measured values of the composite media. These simulations will be run for a range of velocities, to test the reliability of the models and CFD calculations at different operating conditions.

Conclusions

While this study is incomplete, it points to ways to simulate nanofiber additions to filter media, when the nanofibers exist as a single-layer web of interconnected cylindrical elements. We have also developed means to generate fiber cross-sections and size distributions which closely mimic the appearance of SEM images of the cross-sections of actual cellulosic media. CFD runs calculating the pressure drop across the simulated nanofiber web geometry show that the pressure drop across the nanofiber web is a small percentage of the composite media pressure drop.

Acknowledgements

The authors wish to express their appreciation of the help of Christian Candido in converting the domain geometry files generated in this study into formats acceptable to the Fluent CFD code and of Gabriel Justi in creating the mesh of the computational domain. The authors are also grateful to FAPESP, CAPES and CNPq for the financial grants that made this work possible.

References

- Chen D-R., Pui D. Y. H., Hummes D., Fissan H., Quant F. R., Sem G. J. Design and Evaluation of a Nanometer Aerosol Differential Mobility Analyzer (Nano-DMA). *Journal of Aerosol Science*, v. 29, n. 5, p. 497-509, 1998.
- Graham K., Ouyang M., Raether T., Grafe T., Mc Donald B., Knauf P. Polymeric Nanofibers in Air Filtration Applications. Fifteenth Annual Technical Conference & Expo of the American Filtration & Separation Society, Galveston, Texas, April, 2002.
- Longest P. W., Vinchurkar S. Effects of Mesh Style and Grid Convergence on Particle Deposition in Bifurcating Airway Models with Comparisons to Experimental Data. *Medical Engineering & Physics*, v. 29, p. 350-366, 2007.

Podgórski A., Balazy A., Gradón L. Application of Nanofibers to Improve the Filtration Efficiency of the Most Penetrating Aerosol Particles in Fibrous Filters. *Chemical Engineering Science*, v. 61, n. 20, p. 6804-6815, 2006.

Rai M., Yadav A., Gade A. Silver Nanoparticles as a New Generation of Antimicrobials. *Biotechnology Advances*, v. 27, p. 76-83, 2009.

Tronville P., Zhou B., Rivers R. Realistic Air Filter Media Performance Simulation. Part I: Navier-Stokes/Finite-Volume Computational Fluid Dynamics Procedures. *HVAC&R Research*, v. 19, p. 493-502, 2013.

Wang J., Kim S. C., Pui D. Y. H. Investigation of the Figure of Merit for the Filters with a Single Nanofiber Layer on a Substrate. *Journal of Aerosol Science*, v. 39, p. 323-334, 2008.

Warheit D. B., Sayes C. M., Reed K. L., Swain K. A. Health Effects Related to Nanoparticle Exposures: Environmental, Health and Safety Considerations for Assessing Hazards and Risks, *Pharmacology & Therapeutics*, v. 120, n. 1, p. 35-42, 2008.